EFFECT OF FLUID DENSITY ON TWO-PHASE DAMPING FOR PIPING SUBJECTED TO INTERNAL BUBBLY FLOW

C. Béguin, A. Ross & M. J. Pettigrew
BWC/AECL/NSERC Chair of Fluid-Structure Interaction, Department of Mechanical Engineering, École Polytechnique, P.O.Box 6079, succ. Centre-Ville, Montréal (Québec), Canada, H3C 3A7

E. de Langre
Département de Mécanique, Laboratoire d'Hydrodynamique (LadHyX) Ecole Polytechnique, 91128 Palaiseau, France

ABSTRACT

Internal two-phase flow is common in piping systems. Such flow may induce vibration that can lead to premature fatigue or wear of pipes. In the nuclear industry in particular, failure of piping components is critical and must be avoided. Two-phase damping is considered part of the solution, since it constitutes a dominant component of the total damping in piping with internal flow. However, the energy dissipation mechanisms in two-phase flow are yet to be fully understood. The purpose of this paper is to show that two-phase damping in the bubbly flow regime is related to the density difference between phases. A simple analytical model is presented, showing the importance of phase density difference in two-phase damping. Simple experiments are used to verify the relationship between two-phase damping and density difference.

It is known that viscous dissipation due to relative transverse motion between phases may be one important two-phase damping mechanism. From the simple, single bubble model presented here, it is shown that two-phase viscous dissipation increases with the surface area of the bubbles and with density difference between phases.

The experiments are performed with a vertical clamped-clamped tube to verify the effects of fluid densities on two-phase damping. Vegetable oil or air bubbles of controlled diameter are injected in a stagnant liquid (alcohol, water and sugared water) to generate uniform and measurable bubbly flows. Void fraction is regulated by controlling the number of oil or air bubbles. Two-phase damping ratios are obtained from free transverse vibration measurements on the tube.

1. INTRODUCTION

In the nuclear and chemical process industries, many piping elements operate with two-phase flows (Pettigrew and Taylor, 2004). Flow-induced vibration can lead to structural degradation, process malfunction, and component failure. Two-phase damping can significantly contribute to reducing vibration and thus, to prevent premature fatigue or wear. Therefore, it is desirable to identify some of the parameters that govern two-phase damping in pipes with internal two-phase flow.

The first damping experiments in two-phase flow were performed some 25 years ago by Carlucci (1980) on a series of tubes subjected to an axially confined air-water two-phase flow. His results showed that damping in two-phase flow strongly depends on void fraction; no significant relation was found with frequency or fluid mixture velocity. Many researchers have since contributed to the knowledge of two-phase damping.

In the present paper, the effect of density on two-phase damping is investigated. Several two-phase mixture are studied and compared.

2. DAMPING IN TWO-PHASE FLOW

Tube motion affects internal flow and allows energy transfer from tube to fluid and vice versa. If the fluid gains energy, the tube motion is damped; conversely if the fluid looses energy, the tube becomes unstable. Energy transfer is directly related to the initial energy in the fluid and, in particular, kinetic energy. Damping depends a priori on flow rates. Carlucci's experiments and theory show that energy transfer (damping) in two-phase flows is greater than

in single-phase flows. Thus, the concept of two-phase damping was introduced to allow for this difference. The total damping in two-phase flows therefore includes the components of structural (ζ_s), viscous (ζ_v), flow dependent (ζ_f) and two-phase damping ($\zeta_{2\phi}$). Figure 1 shows the contri-

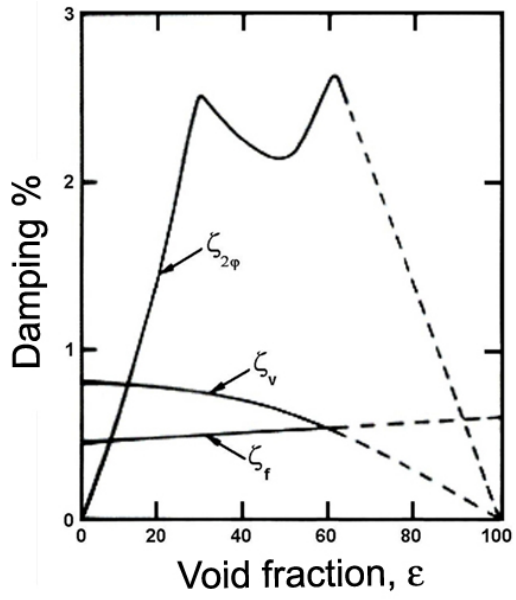

Figure 1: *Components of damping*

bution of each component to the total damping ratio for confined annular air-water axial flow. Structural damping depends on the tube material and supports; it is not shown on this figure. Two-phase damping is preponderant and strongly depends on void fraction. Although Carlucci's tests were performed with an axially confined external flow, the various damping mechanisms in an internal flow are expected to be the same. The geometric configuration is different, but the motion of the tube and the dependence of two-phase damping on void fraction exhibit trends similar to internal flow. Carlucci et al. (1983) suggested that the total damping ratio ζ_t should be given by the sum of the various damping components:

$$\zeta_t = \zeta_s + \zeta_v + \zeta_f + \zeta_{2\phi} \tag{1}$$

3. TEST SECTION AND PROCEDURE

The purpose of the experiments is to measure two-phase damping for two-phase mixtures having different densities. Because two-phase damping may differ in solid-fluid mixtures and fluid-fluid mixtures, all experiment were conducted with fluid-fluid mixtures.

Non miscible fluids with various density differences were selected. Six different mixtures were made using air bubbles or vegetable oil in stagnant alcohol, water and sugared water. To generate a uniform and measurable bubbly flow, the test section shown on Figure 2 was used. The setup was composed of a transparent vertical clamped-clamped tube filled with a stagnant liquid (i.e. alcohol, water or sugared water). The second fluid was injected through a perforated flanged plate at the bottom of the tube. The second fluid was lighter than the stagnant fluid, causing injected bubbles to rise.

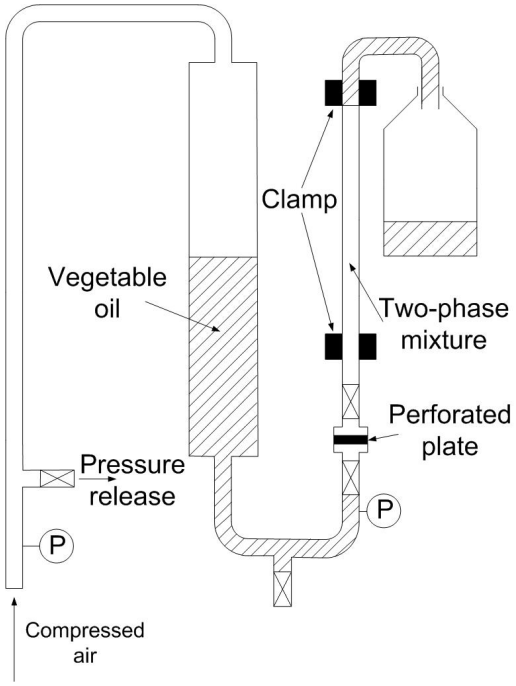

Figure 2: *Test section*

Table 1 presents the dimensions of the oscillating tube. For experiments with oil, compressed air was used to push the oil through the holes of the perforated plate and, thus generate "bubbles". The size of the holes was chosen to provide a "bubble" diameter around 2.5 mm in all mixtures. Experimental results were compared for the same void fractions and "bubble" diameters, in order to maintain the same interface surface area, which is a dominant factor, as previously suggested by Hara (1988) and Gravelle et al. (2007).

Void fraction ε is typically used to characterize the proportion of gas in a two-phase gas-liquid mixture (Collier and Thome, 1996). However,

Length	2.13 m
Internal Diameter	0.0238 m
Internal Volume	3.79 L

Table 1: *Tube dimensions*

Fluid mixture	Densities [kg/m^3] ρ_{hv}	ρ_{lt}	$\Delta\rho$	ρ_{lt}/ρ_{hv}
Sug. Water/Air	1170	1.2	1169	0.10%
Water/Air	969	1.2	968	0.12%
Alcohol 70%/Air	835	1.2	834	0.14%
Sug. Water/Oil	1170	889	281	76%
Water/Oil	969	889	80	92%
Alc.+Wat./Oil	895	889	6	99%

Table 2: *Fluid characteristics* ($\Delta\rho = \rho_{hv} - \rho_{lt}$)

some of the present experiments were conducted with two liquids, and a non-traditional void fraction definition was used :

$$\varepsilon = \frac{V_{lt}}{V_{lt}+V_{hv}} \quad (2)$$

where the subscript '*lt*' is used for the lighter fluid and '*hv*' for the heavier fluid. Void fraction was regulated by controlling the number of oil or air bubbles which depends on the gas pressure, the number and the diameter of the holes. Experiments with air were similar except that compressed air was injected directly through the perforated plate.

Void fraction was determined using two different measurement methods. It was first measured by comparing the volume of the stagnant heavier liquid and that of the two-phase mixture. It was also evaluated from flow rate and "bubble" velocity measurements using :

$$\varepsilon = \frac{Q_{lt}/u_{lt}}{\pi R_t^2} \quad (3)$$

where Q_{lt} is the flow rate of lighter fluid (air or oil) u_{lt} is the "bubble" velocity, R_t is the tube internal radius. The two methods give very similar results.

Table 2 presents the characteristics of fluid mixtures using air, vegetable oil, alcohol, water and sugared water.

Damping was measured using the logarithmic decrement technique with an initial transverse displacement on the tube. Two-phase damping was obtained from the difference between total damping and damping of the tube filled with the higher density fluid.

4. EXPERIMENTAL RESULTS

Two-phase damping was measured for different void fraction and mixture. Figure 3 shows two-phase damping for alcohol-air, water-air and sugared water-air. With these three mixtures, it has been possible to cover a large range of void fractions. The results are plotted for void fractions from 0% to 20%. It was observed that the flow regime was bubbly for void fraction up to 15% in alcohol, 10% in water, 8% in sugared water.

It can be seen as already noticed by Anscutter et al. (2006) that for the low void fractions corresponding to bubbly flow, two-phase damping increases fairly linearly with void fraction.

In bubbly flow, at a given void fraction ε, two-phase damping is greater for heavier stagnant fluid. It is assumed that two-phase damping is due to the relative motion between phases during vibration. Due to the bubble displacement, the stagnant liquid is set into motion, thus acquiring kinetic energy. Damping would then be related to an energy transfer from the tube to the stagnant liquid. The heavier the liquid, the greater is the kinematic energy that could be transfered to it, and the greater is the two-phase damping.

As a consequence of the two preceding remarks, in bubbly flow the gradient of two-phase damping with void fraction is higher with heavier stagnant liquids. However, a drop in two-phase damping occurs at void fractions that correspond to the observed transition to slug flow. This was also observed by Anscutter et al. (2006) and Gravelle et al. (2007) and holds true for all three mixtures. The transition to slug flow occurs at a lower void fraction when the stagnant fluid is heavier. That is why the maximum two-phase damping is lower for heavier stagnant liquids. One possible explanation is that "bubbles" rising faster in heavier fluids have a greater kinematic energy, which possibly stimulates coalescence. But changing fluids involves changing surface tension. Surface tension is known to play a significant role in coalescence, that is why the difference in transition void fraction is possibly due to factors not controled in the present experiments.

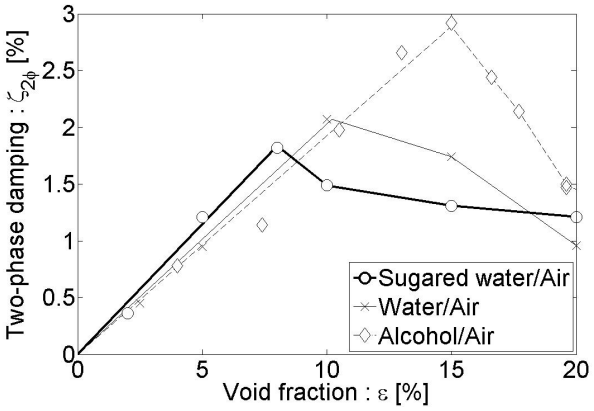

Figure 3: *Two-phase damping for different mixture*

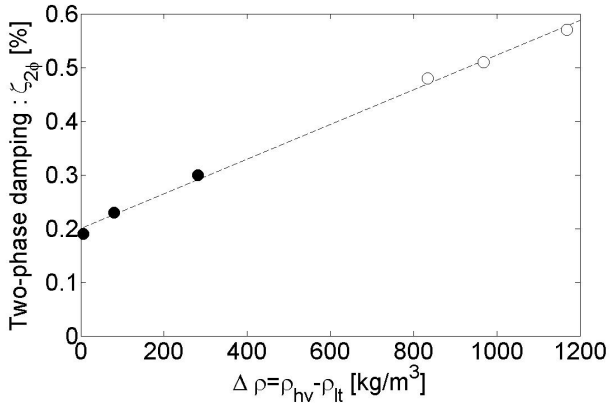

Figure 4: *Two-phase damping of different mixtures at $\varepsilon = 2.5\%$ vs. density difference*

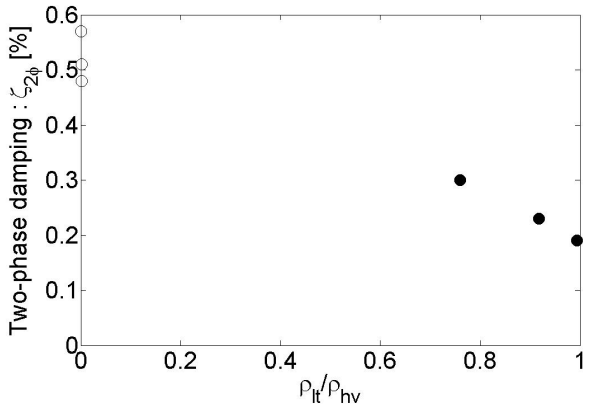

Figure 5: *Two-phase damping of different mixtures at $\varepsilon = 2.5\%$ vs. density ratio*

Figures 4 and 5 show the results of two-phase damping at $\varepsilon = 2.5\%$ for all six fluid mixtures. Interface surface area is known to be a dominant factor for two-phase damping. Therefore, the experimental results are presented for a given void fraction and "bubble" diameter producing the same interface surface area. In Figure 4, two-phase damping is plotted with respect to the density difference $(\rho_{hv} - \rho_{lt})$ between the two fluids. The dashed line shows the fairly linear relationship between two-phase damping and density difference. In Figure 5, two-phase damping is plotted against the density ratio of the two fluids (ρ_{lt}/ρ_{hv}). The three points obtained with vegetable oil in alcohol, water and sugared water (black dots) seem to be fairly linear with density ratio. However, the three points obtained with air bubbles (white dots) contradict this observation. In effect, although the density ratio is very small and almost identical for these three mixtures (ρ_{lt}/ρ_{hv}=0.1% to 0.14%), the two-phase damping values vary greatly (from 0.48% to 0.57%). As a preliminary conclusion, it can be stated that the two-phase damping ratio is relatively well correlated to the density difference between the mixed fluids. The density ratio does not seem to be an adequate parameter to describe two-phase damping.

5. SIMPLE MODEL

A simple analytical model is proposed to show the importance of density difference on two-phase damping. Figure 6 show the geometry of the analytical model. A vertical tube of internal radius R_o is filled with fluid, the secondary phase is represented as a single, non deformable cylindrical bubble. The tube and both fluids are allowed to move in the transverse plane of the tube only. No axial flow or other axial phenomena are considered; thus, there is no effective mass flow through an elementary length of the fluid-filled tube. The primary fluid is allowed to move in any in-plane direction; it is assumed that the primary fluid momentum is conserved in the direction perpendicular to the motion of the tube, and that the motion of the secondary fluid (bubble) is small compared to that of the primary fluid. The equations of motion of the tube (Y coordinate) and bubble (X coordinate) elements are given as:

$$\begin{aligned} M_t\ddot{Y} + C_t\dot{Y} + K_tY &= F_o \\ \rho_{lt}\pi R_i^2\ddot{X} &= F_i \end{aligned} \qquad (4)$$

where M_t, C_t and K_t are the effective mass damping and stiffness per unit length of the tube. To evaluate forces F_o, F_i exerted on the tube and on the bubble, the following hypothesis are

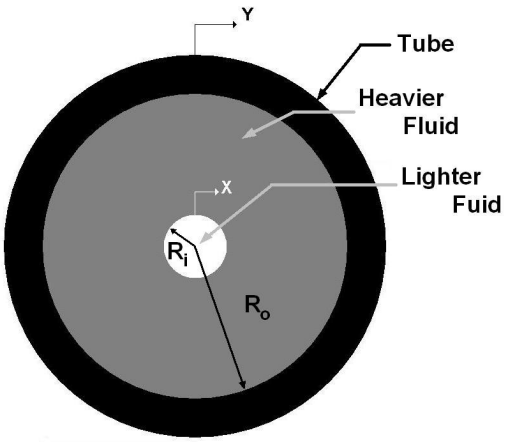

Figure 6: *Geometry of the model*

used. The reference frame is the tube, so inertial forces are added $\rho_{_{hv}}\ddot{Y}\vec{e_x}$. Using polar coordinate in the plane of motion, velocity is given by $\vec{V} = u_r.\vec{e_r} + u_\theta.\vec{e_\theta}$. Navier-Stockes equations are:

$$\begin{array}{l}(a):\\ \frac{\partial u_r}{\partial r} + \frac{u_r}{r} + \frac{1}{r}\frac{\partial u_\theta}{\partial \theta} = 0\\ \\ (b):\\ \frac{\partial u_r}{\partial t} + u_r\frac{\partial u_r}{\partial r} + \frac{u_\theta}{r}\frac{\partial u_r}{\partial \theta} - \frac{u_\theta^2}{r} = -\frac{1}{\rho}\frac{\partial P}{\partial r}...\\ +\nu_{_{hv}}(\frac{\partial^2 u_r}{\partial r^2} + \frac{1}{r^2}\frac{\partial^2 u_r}{\partial \theta^2} + \frac{1}{r}\frac{\partial u_r}{\partial r} - \frac{u_r}{r^2} - \frac{2}{r^2}\frac{\partial u_\theta}{\partial \theta})...\\ +\ddot{Y}cos(\theta)\\ \\ (c):\\ \frac{\partial u_\theta}{\partial t} + u_r\frac{\partial u_\theta}{\partial r} + \frac{u_\theta}{r}\frac{\partial u_\theta}{\partial \theta} + \frac{u_r.u_\theta}{r} = -\frac{1}{\rho}\frac{1}{r}\frac{\partial P}{\partial \theta}...\\ +\nu_{_{hv}}(\frac{\partial^2 u_\theta}{\partial r^2} + \frac{1}{r^2}\frac{\partial^2 u_\theta}{\partial \theta^2} + \frac{1}{r}\frac{\partial u_\theta}{\partial r} - \frac{u_\theta}{r^2} + \frac{2}{r^2}\frac{\partial u_r}{\partial \theta})...\\ -\ddot{Y}sin(\theta)\end{array} \tag{5}$$

where $\nu_{_{hv}}$ is the kinematic viscosity of the heavier fluid. The vorticity equation is deduced from Equations 5-(b) and 5-(c) using $\vec{\nabla} \wedge \vec{V} = \omega\vec{e_z}$ or $\omega = \frac{1}{r}\left(\frac{\partial(ru_\theta)}{\partial r} - \frac{\partial u_r}{\partial \theta}\right)$:

$$\begin{array}{l}\frac{\partial \omega}{\partial t} + u_r\frac{\partial \omega}{\partial r} + \frac{u_\theta}{r}\frac{\partial \omega}{\partial \theta} + ...\\ \underbrace{\omega\left(\frac{\partial u_r}{\partial r} + \frac{u_r}{r} + \frac{1}{r}\frac{\partial u_\theta}{\partial \theta}\right)}_{=0 \quad \text{cf. Equation (5-a)}} = \nu_{_{hv}}\nabla^2\omega\end{array} \tag{6}$$

Using the stream function ψ :

$$\begin{array}{l} u_r = -\frac{1}{r}\frac{\partial \psi}{\partial \theta} \\ u_\theta = \frac{\partial \psi}{\partial r}\end{array} \quad \Rightarrow \quad \omega = \nabla^2\Psi \tag{7}$$

We have :

$$\frac{\partial}{\partial t}(\nabla^2\Psi) - \frac{1}{r}\frac{\partial \Psi}{\partial \theta}\frac{\partial \nabla^2\Psi}{\partial r} + \frac{1}{r}\frac{\partial \Psi}{\partial r}\frac{\partial \nabla^2\Psi}{\partial \theta} = \nu_{_{hv}}\nabla^4\psi \tag{8}$$

Assuming the motion of lighter fluid to be negligible, Equation (8) becomes :

$$\frac{\partial}{\partial t}(\nabla^2\psi) = \nu_{_{hv}}\nabla^4\psi \tag{9}$$

According to the work of Chen (1987) Equation (9) has the following solution :

$$\begin{array}{lcl}\psi & = & (\dot{X} - \dot{Y})G(r)\sin(\theta)\\ \text{with} & & \\ G(r) & = & \frac{A_1}{r} + A_2\ r + A_3\ I_1(\lambda r) + A_4\ K_1(\lambda r)\\ \text{So} & & \\ u_r & = & (\dot{Y} - \dot{X})\frac{G(r)}{r}\cos(\theta)\\ u_\theta & = & (\dot{X} - \dot{Y})G'(r)\sin(\theta)\end{array} \tag{10}$$

where $X = X_0 e^{i\Omega t}$,$\lambda = (i\Omega/\nu_{_{hv}})^{1/2}$. A_1, A_2, A_3 and A_4 are constants that depends on the boundary conditions :

$$\left\{\begin{array}{l} u_r(R_i,\theta) = (\dot{X} - \dot{Y})\cos(\theta)\\ u_\theta(R_i,\theta) = (\dot{Y} - \dot{X})\sin(\theta)\\ u_r(R_o,\theta) = 0\\ u_\theta(R_o,\theta) = 0\end{array}\right. \Rightarrow \left\{\begin{array}{l} G(R_i) = -R_i\\ G'(R_i) = -1\\ G(R_o) = 0\\ G'(R_o) = 0\end{array}\right. \tag{11}$$

The stress tensor is :

$$\bar{\bar{\sigma}} = \left[\begin{array}{cc} -P + 2\mu_{_{hv}}\frac{\partial u_r}{\partial r} & \mu_{_{hv}}\left(r.\frac{\partial \frac{u_\theta}{r}}{\partial r} + \frac{1}{r}\frac{\partial u_\theta}{\partial \theta}\right)\\ \mu_{_{hv}}\left(r\frac{\partial \frac{u_\theta}{r}}{\partial r} + \frac{1}{r}\frac{\partial u_r}{\partial \theta}\right) & -P + \mu_{_{hv}}\frac{2}{r}\frac{\partial u_\theta}{\partial \theta} + \frac{u_r}{r}\end{array}\right] \tag{12}$$

where $\mu_{_{hv}}$ is the dynamic viscosity. Forces are the deduced :

$$\begin{array}{l} df_x(r) = \left[\left(-P + 2\mu_{_{hv}}\frac{\partial u_r}{\partial r}\right)\cos(\theta)\right.\\ \left. ... -\mu_{_{hv}}\left(r.\frac{\partial \frac{u_\theta}{r}}{\partial r} + \frac{1}{r}\frac{\partial u_r}{\partial \theta}\right)\sin(\theta)\right] r d\theta\\ F_x(r) = \int_0^{2\pi} df_x\\ F_i = F_x(R_i) \quad F_o = -F_x(R_o)\end{array} \tag{13}$$

Using Equation (5-c) and integrating by parts for the pressure terms, the forces become :

$$\begin{array}{lcl} F_o & = & \rho_{_{hv}}\pi R_o^2\left[-2A_2\ddot{X} + (2A_2 - 1)\ddot{Y}\right]\\ F_i & = & \rho_{_{hv}}\pi R_i^2\left[(2A_2 + 3)\ddot{X} - (2A_2 + 2)\ddot{Y}\right]\\ & & -2\mu_{_{hv}}\pi(\dot{X} - \dot{Y})\end{array} \tag{14}$$

where A_2 (Equation (11)) only depends on frequency and fluid viscosity. Introducing $2A_2 = b_1 + ib_2/\Omega$ the forces are finally expressed as :

$$\begin{aligned} F_o &= \rho_{hv}\pi R_o^2\left[-\ddot{Y} - b_1(\ddot{X}-\ddot{Y}) - b_2(\dot{X}-\dot{Y})\right] \\ F_i &= \rho_{hv}\pi R_i^2\left[\ddot{X} + (b_1+2)(\ddot{X}-\ddot{Y})\right] + ... \\ &\quad \pi(b_2\rho_{hv}R_i^2 - 2\mu_{hv})(\dot{X}-\dot{Y}) \end{aligned} \tag{15}$$

So the equation of motion (Equation (4)) becomes

$$\begin{aligned} &(M_t + \rho_{hv}\pi R_o^2)\ddot{Y} + C_t\dot{Y} + K_tY = ... \\ &\rho_{hv}\pi R_o^2\left[b_1(\ddot{X}-\ddot{Y}) + b_2(\dot{X}-\dot{Y})\right] \\ &(\rho_{hv}-\rho_{lt})R_i^2\ddot{X} + \rho_{hv}R_i^2(b_1+2)(\ddot{X}-\ddot{Y}) = ... \\ &(2\mu_{hv} - b_2\rho_{hv}R_i^2)(\dot{X}-\dot{Y}) \end{aligned} \tag{16}$$

From Equation (16), it can be seen that an absence of motion between tube and lighter fluid ($X = Y$) implies that the two fluid phases have the same density ($\rho_{hv} = \rho_{lt}$) :

$$\begin{aligned} &(M_t + \rho_{hv}\pi R_o^2)\ddot{Y} + C_t\dot{Y} + K_tY = 0 \\ &(\rho_{hv}-\rho_{lt})R_i^2\ddot{X} = 0 \end{aligned} \tag{17}$$

Since the densities are different ($\rho_{hv} \neq \rho_{lt}$), there must exist a relative motion between the phases. Dissipation would then occur through the following terms :

$$\begin{aligned} &\rho_{hv}R_o^2 b_2(\dot{X}-\dot{Y}) \\ &(2\mu_{hv} - b_2\rho_{hv}R_i^2)(\dot{X}-\dot{Y}) \end{aligned} \tag{18}$$

A complete model would require 3D consideration (spherical bubble rather than cylindrical, vertical velocity of liquid and gas) and confinement (possible interaction between bubble).

6. CONCLUSION

Both the experiments and the model show that the density difference between phases ($\rho_{hv} - \rho_{lt}$) is a major parameter in two-phase damping.

The model also suggests that the liquid viscosity μ_{hv} is of significant importance.

Experiments show also that the difference density ($\rho_{hv} - \rho_{lt}$) may also influence the transition from bubbly flow to slug flow.

Further experiments with perfluorocarbon (high density liquid, non miscible in oil or water) will be carried out to complete two-phase damping data with respect to density difference.

Additional experiments with sugared water and glycerol mixtures (same density but different viscosity) will also be carried out to explore the influence of the viscosity on two-phase damping.

7. ACKNOWLEDGMENT

The experiments reported were performed with the valuable and much appreciated assistance of Caroline Loranger.

8. REFERENCES

Anscutter, F., Béguin, C., Ross, A., Pettigrew, M.J. , Mureithi, N.W., 2006, Two-Phase Damping and Interface Surface Area in Tubes with Internal Flow *Proceedings, ASME Pressure Vessels and Piping Conference 2006* **9** : 537-547.

Carlucci, L.N., 1980, Damping and Hydrodynamic Mass of a Cylinder in Two-Phase Flow. *ASME Journal of Mechanical Design* **102**: 597-602.

Carlucci, L.N., Brown, J.D., 1983, Experimental Studies of Damping and Hydrodynamic Mass of a Cylinder in Confined Two-Phase Flow. *ASME Journal of Vibration, Acoustics, Stress and Reliability Design* **105**: 83-89.

Chen S.S., 1987, Flow-induced vibration of cylindrical structure, *Hemisphere Publishing, New York, NY p30.*

Collier J.G. and Thome J.R., 1996, Convective boiling and condensation, *3rd ed., Clarendon Press, Oxford University Press, p6.*

Gravelle, A. , Ross, A., Pettigrew, M.J. and Mureithi, N.W., April 2007, Damping of tubes due to internal two-phase flow *Journal of Fluids and Structures* **23**(3): 447-462.

Hara, F., 1988, Two-Phase Fluid Damping in a Vibrating Circular Structure *ASME, Pressure Vessels and Piping Division (Publication) PVP* **133** : 1-8.

Harmatty, T.Z., 1960, Velocity of Large Drops and Bubbles in Media of Infinite or Restricted Extend, *AIChE Journal* **6**: 281.

Pettigew, M.J. and Taylor, C.E., November 2004, Damping of Heat Exchanger Tubes in Two-Phase Flow: Review and Design Guidelines. *ASME Journal of Pressure Vessel Technology* **126**: 523-533.